Available online at www.sciencedirect.com

SCIENCE DIRECT®

PERGAMON

International Journal of Multiphase Flow 29 (2003) 375–394

International Journal of Multiphase Flow

www.elsevier.com/locate/ijmulflow

A stochastic model for solid particle dispersion in a nonhomogeneous turbulent field

Ilias Iliopoulos, Yoichi Mito, Thomas J. Hanratty *

Department of Chemical and Biomolecular Engineering, University of Illinois at Urbana-Champaign, 205 Roger Adams Laboratory, Box C-3, 600 South Mathews Avenue, Urbana, IL 61801, USA

Received 9 November 1999; received in revised form 3 December 2002

Abstract

Dispersion of solid particles in three dimensions in a fully developed nonhomogeneous turbulent flow in a channel was studied. A particle point source at a distance of 40 wall units from the bottom wall was considered. Data were obtained by carrying out experiments in a direct numerical simulation. The relative roles of gravity and of turbulence in dispersing the particles are examined. The results are used to test the accuracy of a stochastic Lagrangian model which utilizes a modified Langevin equation to represent the fluid fluctuations seen by a solid particle. All of the parameters, with the exception of the time scales, are obtained from Eulerian statistics. Good agreement is obtained by assuming the spatial variation of the time scales is the same as would be obtained by examining the dispersion of fluid particles. The Langevin equation is further tested by considering the settling of particles that are uniformly distributed in the flow field at time zero. There is some evidence to support the suggestion that the gravitational settling velocity at the wall is greater than the free-fall velocity.

Keywords: Particle dispersion; Settling of particles; Gravitational effect; Langevin equation; Direct numerical simulation; Stochastic modeling

1. Introduction

This paper has two aspects: It presents new results on the behavior of heavy particles in a turbulent fluid flowing through a horizontal channel, that are obtained from experiments in a direct numerical simulation (DNS). It also explores the use of a stochastic method to describe the

* Corresponding author. Tel: +1-217-333-1318; fax: +1-217-333-5052.
E-mail address: hanratty@scs.uiuc.edu (T.J. Hanratty).

0301-9322/03/$ - see front matter
doi:10.1016/S0301-9322(02)00165-9

influence of gravity on turbulent dispersion and deposition of solid particles that originate from a point source in a nonhomogeneous field. The analysis involves the solution of the equation of motion of a solid particle and the modeling of the fluid turbulence seen by the particle by using a modified Langevin equation. The results are compared with the DNS experiments.

The motivation is to describe particle concentration fields in a turbulent flow. The type system of interest is one in which particles are removed from the bottom boundary of a channel through which a fluid is flowing turbulently. These particles have an initial velocity, which is random. Their subsequent behavior is governed by fluid drag and gravity. The particles undergo a turbulent motion and eventually settle at the bottom boundary. The goal is the development of sound theoretical approaches that predict particle concentration profiles in dilute suspensions of drops or of solid particles, such as observed in horizontal gas–liquid annular flows and sediment transport.

The classical approach is to use an Eulerian framework whereby a mass balance equation is applied to a fixed volume in space (O'Brien, 1933; Rouse, 1937). Thus, for fully developed flow in a channel, the concentration distribution, $C(x_2)$, is described by

$$-V_T \frac{dC}{dx_2} = \frac{d}{dx_2}\left[\varepsilon \frac{dC}{dx_2}\right] \tag{1}$$

Here V_T is the free-fall settling velocity and ε is a turbulent diffusivity. Eq. (1), essentially, equates the free-fall velocity to a diffusion velocity associated with the concentration gradient. This approach has a number of flaws: (1) The particles might never reach the free-fall velocity since they are not in the fluid long enough. Furthermore, particles coming off of the bottom boundary would, on average, be moving away from the boundary. (2) The specification of the turbulent diffusivity of the particles, $\varepsilon(x_2)$, does not have a firm foundation. (3) The boundary condition at $x_2 = 0$ needs to be specified empirically.

An alternate approach is to use a Lagrangian framework in which the bottom boundary is considered to consist of a series of sources of particles. The concentration profile is then described as resulting from the net contribution of these wall sources. The main theoretical problems are to describe the behavior of one of these sources and to develop a physical understanding of how particles are lifted from the bottom boundary. This paper addresses the first of these problems.

The Lagrangian approach outlined above has been applied by Binder and Hanratty to vertical gas–liquid annular flow (1991), to horizontal gas–liquid annular flow (1992) and to sediment transport (1993). The flow field was homogeneous, the particles were assumed to enter the field with a velocity that is proportional to the friction velocity. The concentration profiles of particles originating from a source at time zero were calculated as a function of time by a deterministic differential equation, motivated by Taylor's theory of diffusion from a source in a homogeneous isotropic field. These works have a kinship to an analysis by Hunt and Nalpanis (1985) which represents concentration profiles in the saltation regime as the result of a series of deterministic particle trajectories that originate from the bed surface. In a sense, they extend the saltation analysis so as to include nondeterministic effects of turbulent diffusion.

The present paper explores an improved method for describing the behavior of a source, by considering the nonhomogeneity of the field and by directly accounting for the stochastic behavior of the particles. The system considered is fully developed turbulent flow in a channel. The source of particles is located at a distance of 40 wall units from the bottom wall, where a wall unit is

defined as the ratio of the kinematic viscosity to the friction velocity. The particles are assumed to have the same velocity as the fluid at time zero. The Eulerian properties of the fluid turbulence are obtained from a DNS. The use of $x_2 = 40$ as the source location was motivated by a desire to examine conditions for which nonhomogeneities of the turbulence are playing an important role. Furthermore, for most systems of interest, the viscous wall region is negligibly thin, so $x_2 = 40$ is essentially at the wall. The Langevin equation developed in these studies is tested by considering the settling of solid particles which are uniformly distributed over the flow field. This is done by adding the contributions from a distribution of instantaneous sources.

The equation of motion of the solid particles is solved exactly in a computer experiment, in which the fluid velocity at the particle position is supplied by a DNS. In the stochastic model, the solid particle equation of motion is the same as in the computer experiment, but the fluid velocities seen by the solid particles are modelled with a modified Langevin equation.

The computer experiment clearly shows an Eulerian approach such as Eq. (1) does not capture the influence of the previous history of the diffusing particles. However, the Lagrangian approach should address the central problem that the time variation of the statistical properties of the fluid velocity seen by the diffusing particles is different from the time variation of diffusing fluid particles because inertial and gravitational effects cause the solid particle to become disengaged from the fluid particle in which it is immersed. A theoretically sound solution to this problem is not available for fields which are neither homogeneous nor isotropic. The approach taken in this paper is to argue that the problem of accounting for the effects of turbulence nonhomogeneities is of primary importance and that the representation of the time variation of the turbulence seen by the solid particle can be approximated from studies of the dispersion of fluid particles. We use the Langevin equation to represent the fluid turbulence because previous work has demonstrated its ability to capture the effects of nonhomogeneities (Iliopoulos and Hanratty, 1999). The time constant in the Langevin equation can be adjusted to take account of the inability of heavy particles to follow exactly fluid particles. (However, it was found that this was not necessary.) The approach described above has previously been explored by Perkins (1992) in his study of dispersion of heavy particles in a turbulent jet. It is further discussed in a paper by Pozorski and Minier (1998).

2. Dispersion in a homogeneous turbulence

Most of the theoretical work on dispersion of spherical particles from a point source has considered a homogeneous isotropic field, for which the mean velocity is zero. Friedlander (1957) solved the equation of motion,

$$\frac{\mathrm{d}\vec{v}}{\mathrm{d}t} = \beta(\vec{u} - \vec{v}) \tag{2}$$

where $\vec{v}$ is the particle velocity, $\vec{u}$ is the randomly varying fluid velocity and β is the reciprocal of the inertial time constant, defined as

$$\beta = \frac{1}{\tau_\mathrm{p}} = \frac{3}{4}\frac{C_\mathrm{D}\rho_\mathrm{f}}{d_\mathrm{p}\rho_\mathrm{p}}|u_\mathrm{s}| \tag{3}$$

Here d_p is the particle diameter, $\rho_p$is the particle density, ρ_f is the fluid density, C_D is the drag-coefficient and $|u_s|$ is the magnitude of the slip velocity (fluid minus particle velocity). The dimensionless inertial time constant of the particle, $\tau_p^+ = u^{*2}/v_f\beta$, expresses the ratio of the drag force of the carrier fluid to the inertia of the particles. It is also a measure of the stopping distance of a particle in a still fluid to the thickness of the viscous wall layer. Friedlander showed that under stationary conditions the dispersion of particles in a homogeneous isotropic field can be characterized by a turbulent diffusivity, defined as

$$\varepsilon_p = \overline{u^2}\int_0^\infty R(\theta)\,\mathrm{d}\theta \tag{4}$$

where θ represents time and the correlation $R(\theta)$ is different from the Lagrangian or the Eulerian velocity correlation coefficients defined for the fluid. It represents the correlation of the fluid velocities seen by the particles, whose paths are unknown. For an approximation by an exponential function $R(\theta) = \exp(-\alpha\theta)$ the turbulent diffusion coefficient is

$$\varepsilon_p = \frac{\overline{u^2}}{\alpha} = \frac{\varepsilon_f}{\alpha\tau_{LF}} \tag{5}$$

where τ_{LF} is the Lagrangian timescale of the turbulence and ε_f is the diffusivity of the fluid. The ratio of the velocity fluctuations of the solid particles to the velocity fluctuations of the fluid is given as

$$\frac{\overline{v^2}}{\overline{u^2}} = \frac{\beta\tau_{LF}}{\alpha\tau_{LF} + \beta\tau_{LF}} \tag{6}$$

For large β (small particle inertia) $\overline{v^2} = \overline{u^2}$. However for small β (large particle inertia) $\overline{v^2}$ can be much smaller than $\overline{u^2}$. The evaluation of $R(\theta)$ presented a challenging theoretical problem, which was solved by Reeks (1977) and by Pismen and Nir (1978) for a homogeneous, isotropic field, by an iterative approach.

3. Dispersion in a nonhomogeneous field

3.1. Model for particle motion

A simplified equation of motion of a solid particle which includes only drag and gravity forces is considered. The fluid velocity, $\vec{U}$, is the sum of an average and a fluctuating component. The velocity of a particle, $\vec{V}$, is obtained by integrating the following equation:

$$\frac{\mathrm{d}\vec{V}}{\mathrm{d}t} = -\frac{3}{4}\frac{\rho_f C_D}{d_p\rho_p}|\vec{V} - \vec{U}|(\vec{V} - \vec{U}) + \vec{g}\left(1 - \frac{\rho_f}{\rho_p}\right) \tag{7}$$

where $\vec{g}$ is the acceleration of gravity and $g_2 = -g(g > 0)$, $g_1 = g_3 = 0$. The subscripts 1, 2, 3 indicate the streamwise, wall-normal and spanwise components. The drag-coefficient is given by the following expression (Clift et al., 1978):

$$C_D = \frac{24}{Re}(1 + 0.15Re^{0.687}) \tag{8}$$

where Re is the particle Reynolds number defined with the particle diameter and the magnitude of the relative velocity $|\vec{V} - \vec{U}|$. The equation of motion for the particles includes the effect of nonlinearities on the fluid drag but does not include the effects of lift.

Eq. (7) is to be solved for particles originating at $t = 0$, $\vec{x}_0$ with some specified velocity $\vec{V}_0$. The change of the location of a particle over some time interval, dt, is given by

$$\frac{d\vec{x}}{dt} = \vec{V} \tag{9}$$

The velocity of the fluid, encountered by the particle, $\vec{U}(\vec{x}, t)$ is a random function. The solution of Eqs. (7) and (8) for a typical $\vec{U}(\vec{x}, t)$ gives a possible realization of $\vec{V}(\vec{x}, t)$ and $\vec{x}(t)$. Dispersion is calculated by considering the average of a large number of trajectories. The principal problem is the specification of $\vec{U}(\vec{x}, t)$ from a knowledge of the Eulerian or Lagrangian statistics describing the fluid turbulence.

3.2. Stochastic model for dispersion of fluid particles

The starting point for the execution of the analysis outlined above is the development of a stochastic representation of the dispersion of fluid particles. The classical paper by Taylor (1921) describes the statistical behavior of a large number of fluid particles originating from a point source in a homogeneous, isotropic turbulent field. The Langevin equation produces the same results as Taylor's analysis if the correlation coefficient is given as $R = \exp(-t/\tau_L)$, where τ_L is the Lagrangian time scale. However, it has the advantage that it can be used in more complicated flows, so a number of investigators have explored ways to adapt it to nonhomogeneous fields (Durbin, 1983, 1984; Hall, 1975; Legg and Raupach, 1982; Reid, 1979; Reynolds, 1997; Thomson, 1984, 1986, 1987).

The approach taken in this paper is close to that suggested by Thomson. It is described in a thesis by one of the authors (Iliopoulos, 1998) and in a recent paper by Iliopoulos and Hanratty (1999). The fluid velocity is defined as the sum of the Eulerian average, $\bar{U}_i(x_2)$, and a fluctuation u_i. For a fully developed flow, the following stochastic equation is used to represent a possible change of the components of $\vec{u}$ along the trajectory of a fluid particle:

$$d\left(\frac{u_i}{\sigma_i}\right) = -\frac{u_i}{\sigma_i \tau_i}dt + d\mu_i + \bar{A}_i dt \tag{10}$$

where $\bar{A}_i dt$ represents the average of random forcing functions for a large number of trajectories, and $d\mu_i$ is a random variable with zero mean. Repeated indices do not imply summation. The Eulerian root-mean-square of u_i is designated by σ_i and

$$\bar{A}_i = \frac{\partial\left(\frac{\overline{u_2 u_i}}{\sigma_i}\right)}{\partial x_2} \tag{11}$$

For homogeneous isotropic turbulence, σ_i and τ_i are constants, $\bar{A}_i = 0$ and τ_i is the Lagrangian timescale τ_L. For inhomogeneous flow σ_i and τ_i are allowed to vary with x_2 and $\bar{A}_i \neq 0$.

Expressions for the moments of $\overline{\mathrm{d}\mu_i^n}$ are given by Iliopoulos and Hanratty (1999). For example, the ensemble averages of covariances of $\mathrm{d}\mu_i$ are given as

$$\overline{\mathrm{d}\mu_i \mathrm{d}\mu_j} = \left\{ \frac{\partial \frac{\overline{u_i u_j u_2}}{\sigma_i \sigma_j}}{\partial x_2} + \frac{\overline{u_i u_j}}{\sigma_i \sigma_j} \left(\frac{1}{\tau_i} + \frac{1}{\tau_j} \right) \right\} \mathrm{d}t + \mathrm{o}(\mathrm{d}t)^2 \tag{12}$$

The spatial variation of $\sigma_i(x_2)$ is obtained from the measured or calculated Eulerian properties of the turbulence. The time scales τ_i can be rigorously defined only for homogeneous isotropic turbulence. Researchers have interpreted τ_i as the local decorrelation rate, that is, the persistence of motion in a certain direction. However its exact definition is unclear.

The results presented in this paper are for the single case of a fully developed flow. As mentioned earlier, they can find direct application in developing methods to predict entrainment in horizontal fully developed annular flows (Pan and Hanratty, 2002). However, they could also be a starting point for analyzing more complicated flows. More general formulations are given by Thomson (1986) for a Gaussian forcing function and by Reynolds for a skewed forcing function (1997). For three-dimensional flows, a formulation of the Langevin equation which models the instantaneous total velocity, $U_i = \overline{U}_i + u_i$, rather than u_i (Pope, 1994), could be a more attractive approach. Time scales, both in simple and complex flows, have been defined as equal to $2\sigma_i^2/C_0\varepsilon$, where ε is the dissipation of turbulent energy (Tennekes, 1979). Sawford (1991) suggested $C_0 = 7$ and Du et al. (1995) suggested $C_0 = 3 \pm 0.5$ from experiments done in a homogeneous, isotropic field.

3.3. Stochastic model for fluid turbulence seen by the solid particles

As discussed in Section 2 the solid particles do not follow the fluid particles so a fundamental problem is how to take this into account. An approach which has been explored by a number of investigators is to use two step stochastic models. Over a given time interval the displacement of the particle and of the fluid particle with which it is in contact are calculated.

A stochastic model is used to specify a new velocity for the fluid particle. The fluid particle and the solid particle end up at different locations since they had different velocities at the beginning of the time interval, $\mathrm{d}t$. Therefore a method needs to be developed to relate the velocity of the fluid in contact with the particle to the new velocity specified for the displaced fluid element. This has been done by using a spatial correlation function. As pointed out in an extensive review by Pozorski and Minier (1998), theoretical justification for this approach has not been developed. A recent work by Ushijima (Ushijima, 1998; Ushijima and Perkins, 1998) presents evidence that the use of an Eulerian space correlation in a two step analysis is fundamentally wrong. Furthermore, the method for implementing the two-step model in a nonhomogeneous field is not obvious.

Therefore, the much simpler approach of using Eq. (10) to describe the velocity of the fluid seen by the particle has been taken. The time constant might need to be adjusted to take account of the discrepancy between the velocity history of fluid particles and the velocity history of the fluid seen by solid particles along a trajectory. The expectation is that τ_i could depend on a dimensionless inertial time constant of the solid particles and a dimensionless free-fall velocity. The motivation is that it is more important to capture effects of nonhomogeneities of the fluid turbulence than to describe exactly the consequences of the solid particle not following a fluid particle. That is, the

results of the analysis will be forgiving of errors in specifying $\tau_i(x_2)$. Furthermore, the analysis is much easier to execute than is a two step stochastic model.

4. Studies in a DNS of turbulent flow in a channel

4.1. Description of studies of dispersion from a point source

All results are presented in nondimensional form using the friction velocity and the kinematic viscosity. The system considered is fully developed flow between two horizontal smooth walls, separated by a distance $2H$, that extends to infinity in the streamwise and spanwise directions. The Reynolds number, based on the average fluid velocity and the distance between the planes, $2H$, is 4520. Dimensionless H equals 150. The three-dimensional, time-dependent fluctuating velocity field was obtained by solving numerically the Navier–Stokes and continuity equations in a three dimensional grid, as described by Lyons et al. (1991). The computational volume had dimensions of 1900 and 950 in the x_1 and x_3 directions. A periodic boundary condition was used in the x_1 and x_3 directions. The number of grid points was $128 \times 65 \times 128$. The resolution in the x_2 direction varied from 0.18 at the wall to 7.4 at the center of the channel. The resolutions along the other coordinates were $\Delta x_1 = 15$ and $\Delta x_3 = 7.4$. The computational time step was 0.25.

Particles were released at $x_2 = 40$ with the same velocity as the fluid. For each particle, the change of velocity and of position with time was calculated with Eqs. (7) and (9). The first-order Euler explicit method was used for the first time step. Then the second-order Adams–Bashforth method was used. The fluid velocity appearing in Eq. (7), was obtained from the DNS by using an interpolation scheme developed by Kontomaris et al. (1992). A particle deposited on the wall when it hit the wall. Statistics were calculated by averaging results from 16129 particle paths. This simulation was performed over a time period of 400.

Conditions were selected so as to have an inertial time constant ($\beta\tau_{LF} = 1.7$) that permits the particles to follow the turbulence reasonably well over most of the flow field, when there is no gravitational field, and a ratio of stopping distance to the thickness of the viscous wall layer ($\beta^{-1} = 20$) that allows the particles to move through a region close to wall by free-flight (McCoy and Hanratty, 1977). This was accomplished by using a particle radius of $d_p/2 = 0.18$ and a ratio of particle to fluid density of $\rho_p/\rho_f = 2650$. The Froude number, $u^{*2}/2\tilde{g}\widetilde{H}$, was 0.145, where $\tilde{g}$ and $\widetilde{H}$ have dimensions. Then, $g = 1/2\ \mathrm{Fr}H = 0.023$, $V_T = \beta^{-1}g(1 - \rho_f/\rho_p) = 0.46$. The Lagrangian time scale, τ_{LF}, used in these characterizations was calculated with a relation given by Vames and Hanratty (1988), $\varepsilon_f = 0.037\,D$, where ε_f is the dimensionless turbulent diffusion coefficient and D is the dimensionless pipe diameter. By substituting the hydraulic diameter of the two dimensional channel ($4H$) for D, the Lagrangian time scale is calculated as $t_{LF} = 35$ by using the dimensionless turbulent intensity, 0.8.

4.2. Results for dispersion from a point source

This section presents DNS results for dispersion of solid particles originating from $x_2 = 40$ and discusses, in a few places, results for dispersion of fluid particles that have been presented in a previous article by Mito and Hanratty (2002). The latter will be referenced as MH.

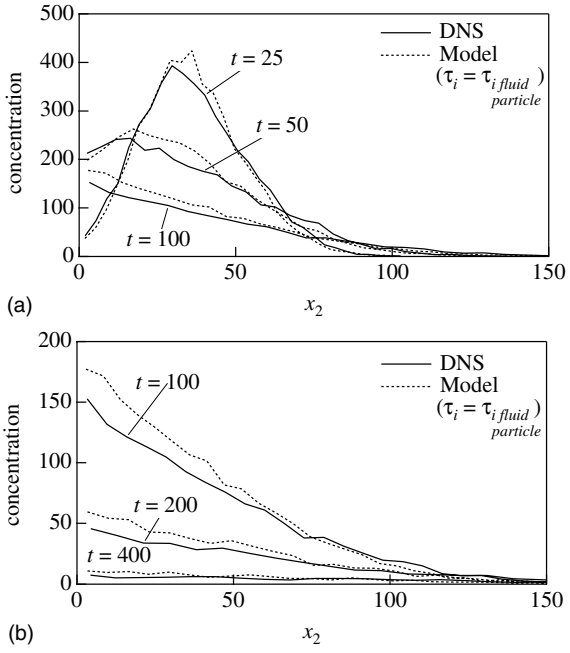

Fig. 1. Distribution of solid particles in the wall-normal direction.

Concentration profiles of solid particles are plotted in Fig. 1 as solid curves. The 16129 particles spread as a cloud in the x_1, x_2 and x_3 directions. The region where the particles were located was divided into 30 bins, equally spaced in the x_2 direction. The number of particles in each bin is divided by Δx_2 to give a concentration.

At $t = 0$ all the solid particles are located at $x_2 = 40$. As time proceeds the particles spread out. The maximum in the concentration decreases and moves toward the wall with increasing time. At large enough times the maximum exists at the wall. Particles deposit on the wall and the number of particles in the flow field decreases with time. Eventually all the particles deposit and the concentration becomes zero everywhere. A plot of the number of particles in the field as a function of time is given in Fig. 2a as a solid curve. Results on the rate of deposition are presented Fig. 2b. From Fig. 2b it is seen that deposition doesn't begin to occur until $t \cong 10$. The rate reaches a maximum at $t \cong 65$. The decrease in the rate after this largely reflects a decrease in the concentration at the wall since the rate is equal to the product of the concentration and the average velocity of the particles $\langle V_2 \rangle$ close to the wall.

This is illustrated in Fig. 3 where the average dimensionless values of the velocity of the particles depositing on the wall are presented. The dashed line represents the free-fall velocity, $V_2 = -V_T (= -0.42)$. For $t < 10$ no solid particles reach the wall. For times slightly greater than this V_W has a larger magnitude than V_T. Particles are striking the wall because of their turbulence. They have very large velocities and are launched toward the wall from locations near $x_2 = 40$. For large times, V_W reaches an approximately constant value, which is larger than V_T, indicating that both particle turbulence and gravity are having an effect. In this region dN/dt varies mainly because of variations in the concentration near the wall.

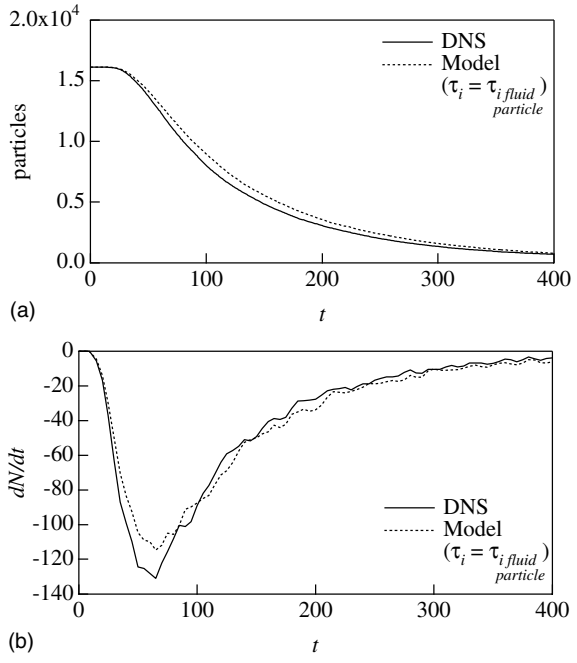

Fig. 2. (a) Particles remaining in the flow. (b) Rate of deposition of particles.

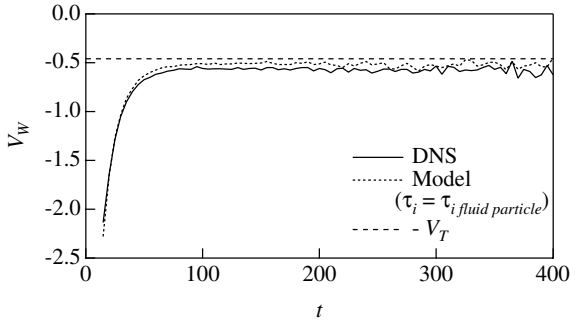

Fig. 3. Average velocity of particles depositing on the wall.

Mean values of the velocity of the particles in a direction perpendicular to the wall, conditional on the particle positions and the times, $\langle V_2 \rangle$, are given in Fig. 4. The values of $\langle V_2 \rangle$ close to the wall and V_W can be different because these averages represent different populations, in that $\langle V_2 \rangle$ represents all the particles at a given location not just those which are hitting the wall. The horizontal dashed line represents the free-fall velocity. A similar plot for fluid particles is given by MH. In this case the mean velocity represents a turbulent flux that results because of the existence of concentration gradients; it is zero for large enough times when concentration gradients are small. For solid particles the mean values of V_2 show the additional influence due to the gravitational

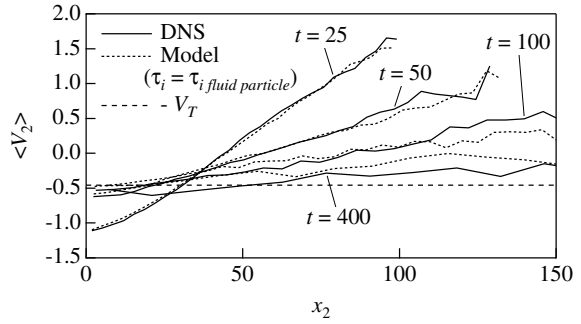

Fig. 4. Ensemble averages of wall-normal velocities of solid particles conditional on the particle positions.

field, which persists for large times. However, it is noted that the mean velocity can be different from the free-fall velocity, even for large times.

For $t = 25$ the mean velocities of solid particles mainly represent turbulent fluxes. At the location of the maximum in the concentration the flux is zero. It is positive for $x_2 > 40$ where the concentration gradients are negative. For large t gravitational settling becomes more important. The location of zero flux moves to larger x_2 and no longer corresponds to the maximum in the concentration profile. It is noted that at large x_2 the mean value of V_2 can be positive. This indicates that the flux of these particles is dominated by turbulent diffusion.

The dispersion of particles in the flow direction is depicted in Fig. 5. This was calculated by using 30 equispaced bins distributed in the region where the particles were located. The concentrations represent the number of particles distributed in the x_3 and x_2 directions for a given x_1. The solid particles are convected downstream by the mean flow and the turbulence. The distribution is symmetric for $t \leqslant 25$. At later times particles which accumulate close to the wall, where the velocity is small, tend to lag behind particles farther away from the wall. Consequently, asymmetric profiles with longer tails develop.

Results on the streamwise velocity fluctuations are presented in Fig. 6. The ordinate is the root-mean-square of the difference between the instantaneous streamwise velocity and the local mean velocity. The curves created with dots and dashes give the Eulerian values of $(\overline{u_1^2})^{1/2}$. In the study of the dispersion of fluid particles (MH) the streamwise velocity fluctuations approach the Eulerian values at large times for all x_2. The solid particles show $(\overline{v_1^2})^{1/2}$ that are only slightly lower than the Eulerian values for $x_2 > 15$ and large t. However, an interesting behavior for $x_2 < 15$ is observed for solid particles in that the values of $(\overline{v_1^2})^{1/2}$ are much larger than $(\overline{u_1^2})^{1/2}$. This result is not anticipated from theories for homogeneous isotropic turbulence. It can be understood by recognizing that the particles move from regions where the mean and fluctuating velocities of the fluid are high to regions where they are low without having the time to adjust to the new environment. This enhancement of streamwise velocity (fluctuations) of the solid particles in the presence of gradients of the mean fluid velocity could be a general behavior, as pointed out by Lillegren (1993).

Results for the root-mean-square of the spanwise component of the particle velocity fluctuations are presented in Fig. 7. Over most of the flow field they are seen to be less than the Eulerian fluid velocity fluctuations. This is consistent with measurements of $\overline{v^2}$ represented by Eq. (6).

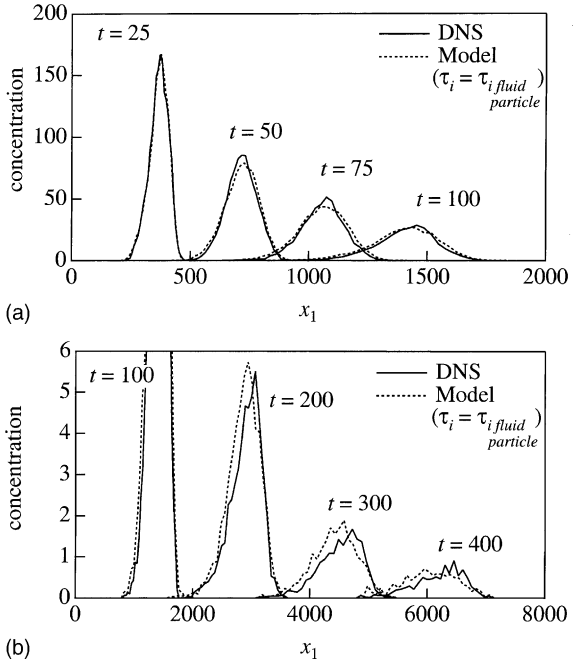

Fig. 5. Distribution of solid particles in the streamwise direction.

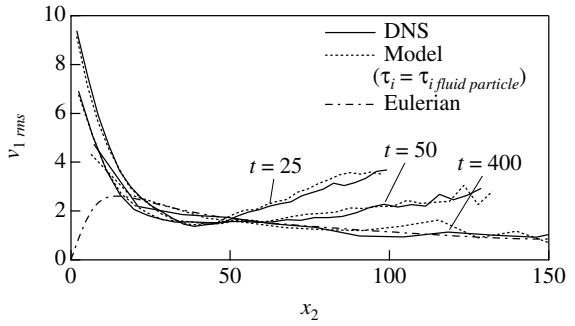

Fig. 6. Ensemble root-mean-squares of streamwise velocity fluctuations of solid particles conditional on the particle positions.

These indicate that the inertia of the particle ($\beta\tau_{\mathrm{LF}} = 1.7$) is large enough that particles do not follow the fluid turbulence exactly.

The intensities of the wall-normal and streamwise fluid velocity fluctuations seen by the particles are given in Fig. 8a and b. The line created with dots and dashes represents the Eulerian values. Within the statistical accuracy of the calculations, the intensities of velocity fluctuations seen by the particles equals the Eulerian intensities at large enough times.

Lagrangian correlations of the fluid velocity fluctuations seen by the particles are presented in Fig. 9. Since the flow is nonhomogeneous, the correlation at time t is normalized by the values of

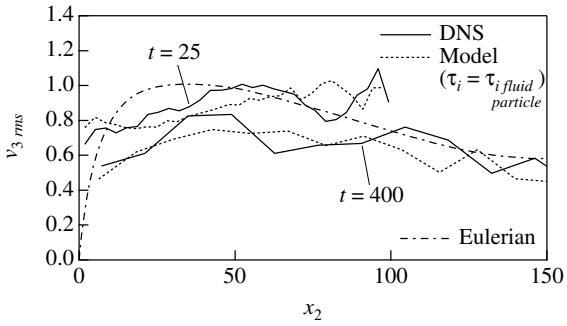

Fig. 7. Ensemble root-mean-squares of spanwise velocity fluctuations of solid particles conditional on the particle positions.

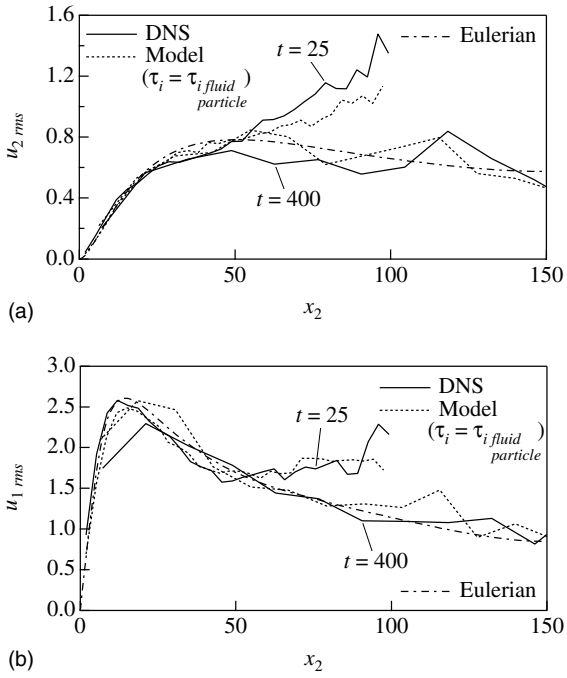

Fig. 8. (a) Ensemble root-mean-squares of wall-normal fluid velocity fluctuations seen by solid particles conditional on the particle positions. (b) Ensemble root-mean-squares of streamwise fluid velocity fluctuations seen by solid particles conditional on the particle positions.

the rms velocities at time 0 and at time t; i.e., $\langle u_i(0)u_i(t)\rangle / \langle u_i^2(0)\rangle^{1/2}\langle u_i^2(t)\rangle^{1/2}$. Thus R_{ii} does not assume values greater than unity.

Plots of the Lagrangian correlation coefficients for all of the solid particles that are in the field at time t are given in Fig. 10. It is noted that R_{22} drops below zero. This is because the gravitational field causes the solid particles to assume a negative V_2 approximately equal to V_T, at large

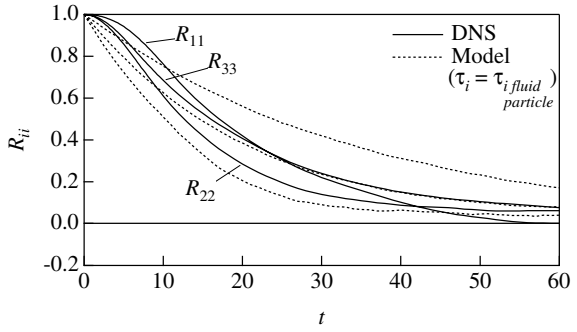

Fig. 9. Lagrangian correlation of fluid velocity fluctuations seen by solid particles.

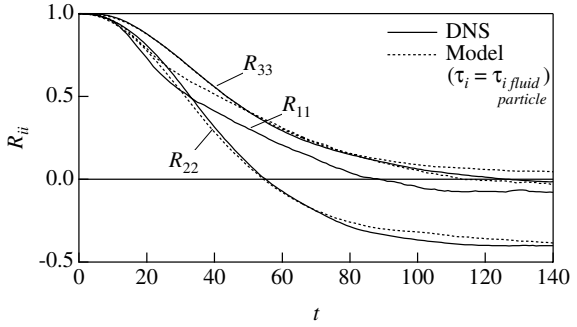

Fig. 10. Lagrangian correlation of velocity fluctuations of solid particles.

times. Solid particles that had negative velocities at $t = 0$ have a small chance to be in the field at large t. Therefore, particles which have a negative settling velocity at large t most likely had a positive V_2 at time zero.

5. Results for stochastic calculation of dispersion from a point source

5.1. Implementation of the stochastic model

Eqs. (7) and (9) were solved to obtain the changes of the velocity and the position of a solid particle with time. At zero time the particle velocity and the fluid velocity were selected to be the same as used in the experiments in the DNS. The fluid velocity is defined as the sum of the Eulerian average, $\overline{U}_i(x_2)$, and a fluctuation u_i. The changes of u_i with time are given by Eq. (10).

An Adams–Bashforth explicit scheme, that is accurate to second-order, was used to solve Eqs. (7) and (9). The Euler explicit method, which is first-order accurate, was used for the first time step. Eq. (10) was discretized with the fully implicit method. The timestep was the same as was used in calculations of particle paths in the DNS.

Mito and Hanratty (2002) showed that the use of a joint Gaussian forcing function in the modified Langevin equation greatly improves the calculations of dispersions, mean velocities and turbulence quantities in a nonhomogeneous field. Therefore, a random variable $d\mu_i$ in Eq. (10) was specified by a joint Gaussian function with $\overline{d\mu_1^2}$, $\overline{d\mu_2^2}$, $\overline{d\mu_3^2}$, $\overline{d\mu_1 d\mu_2}$ given by Eq. (12). The assumption of Gaussianity for the random forcing function implies a velocity field with Gaussian turbulence. Thus the triple correlations in Eq. (12) were taken to be zero. The assumption of a correlation for the random variables in Eq. (10) enables the calculation to include the effect of $\overline{u_1 u_2}$ which plays an important role in transport phenomena in nonhomogeneous fields.

5.2. Results for dispersion from a point source

Fig. 11 presents the characteristic time scales that were used by MH to calculate dispersion of fluid particles with the modified Langevin equation. These were used to represent the fluid turbulence seen by the solid particles. Approximate support for this choice is obtained from Fig. 9 where the calculated correlation coefficients of the fluid particle fluctuations seen by the particles roughly agree with the DNS experiments for R_{22} and R_{33}. However, this is not the case for R_{11} where the comparison is suggesting that values of τ_1 should be smaller than those presented in Fig. 11. A number of calculations were done in which all three time scales were increased or decreased and in which τ_2, τ_3 were kept the same and τ_1 was decreased. Significant improvements could not be recognized so the simple procedure of using time scales obtained from a representation of fluid particle dispersion was chosen.

Calculated concentration profiles, presented in Fig. 1, are seen to be in reasonable agreement with the DNS experiments. As shown in Fig. 2a the comparison of the calculated number of particles remaining in the field with the DNS is reasonably good. However the results from the model are slightly larger. This partially accounts for the differences in the concentration profiles shown in Fig. 1. A comparison of the rates of deposition is given in Fig. 2b. The calculated magnitudes are seen to be smaller than the values obtained with the DNS for $10 < t < 100$. This accounts for the differences shown in Fig. 2a. The results shown in Figs. 3 and 4 indicate that deposition in this range of t is associated with particles that have large velocities and that start free-flights to the wall at a distance from the wall. The lower deposition rates predicted by the

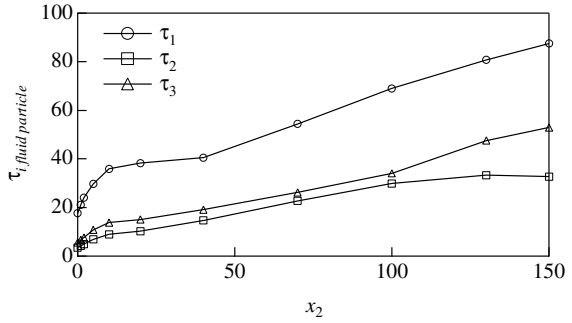

Fig. 11. Time scale variation of fluid particles with the distance from the wall.

model seem to suggest the number of particles launched toward the wall is larger than is predicted by a Gaussian forcing function. For $t > 100$ the calculated rates of deposition are slightly larger than what is observed in the DNS experiments. This probably is a consequence of the larger concentrations of particles predicted to exist at the wall.

Calculated values of the mean velocity in the wall-normal direction, shown in Fig. 4, are in good agreement with the DNS. The values of the magnitude of $\langle V_2 \rangle$ at the wall are seen to be slightly smaller for the model. This is consistent for the differences in dN/dt seen in Fig. 2b.

Calculated concentration profiles in the x_1-direction are compared with the DNS in Fig. 5. The agreement is quite good.

The calculated root-mean-square of the velocity fluctuations in the streamwise direction, shown in Fig. 6, agree with the DNS values. As seen in Fig. 7, both the model and the DNS show values of the spanwise root-mean-square of the velocity fluctuations, at large times, which are smaller than the Eulerian values. Fig. 8a and b present values of the root-mean-square of the fluid velocity fluctuations seen by the particle. Both the model and the DNS produce values that are approximately in agreement with Eulerian results. The predicted values of the Lagrangian correlation coefficients, shown in Fig. 10, agree with the DNS. This agreement is particularly striking for R_{22} and R_{33}.

6. Results for dispersion of uniformly distributed particles

6.1. Description of DNS

A calculation was carried out to examine the settling of uniformly distributed particles in a horizontal turbulent channel flow. This was done with the same flow field and solid particles that were used in the DNS study of dispersion from a point source. The channel was filled with 27×10^4 solid particles which had the same velocity as the fluid at time zero, so that there was a uniform distribution of sources. The simulation was performed over a time period of 500.

6.2. Implementation of stochastic model

The Langevin Eq. (10) was also used to calculate the settling of uniformly distributed particles in the horizontal turbulent channel flow. The numerical method was the same as described in Section 5.1. The characteristic time scales of fluid particles, shown in Fig. 11, were used. The initial conditions were selected to be the same as used in the DNS experiment.

6.3. Results

Time variation of the concentration profiles of the solid particles is given in Fig. 12. A bin size of $\Delta x_2 = 10$ was used for the sampling. Results from the DNS experiment are represented by solid curves and results from the model calculation are represented by dotted curves. At time zero the concentration is uniform, as represented by the dashed line. The particles tend to move toward the bottom wall due to the gravitational force. This causes steep gradients of the concentration

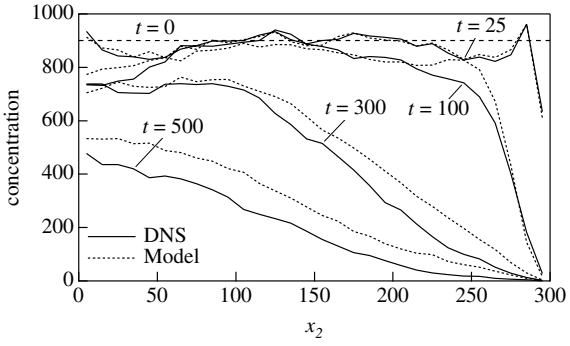

Fig. 12. Distribution of uniformly distributed solid particles in the wall-normal direction.

profiles near the top wall. At small times the particles redistribute, mainly, by turbulence. The minima that appear close to the top and bottom walls at $t = 25$ result from a turbophoretic effect, whereby particles move from regions of high turbulence to regions of low turbulence.

As time proceeds gravity plays a more important role. At $t = 100$ the concentration is observed to decrease markedly near the top wall. However, the effects of nonhomogeneities in the turbulence can be still be noted. At $t = 500$ the particles are observed to have a maximum at the bottom wall and to decrease monotonically with increasing x_2.

The model is seen to agree with the DNS results at $t = 25$. However, at $t = 100$ and 300, the model shows larger concentrations of particles than the DNS at large values of x_2. These results suggest that the model is predicting that gravitational settling is opposed by larger turbulence at large x_2 than is observed in the DNS. At large times the particle concentration close to the wall is observed to decrease more rapidly in the DNS calculations than in the model calculations. The model appears to be underpredicting the influence of turbulence in depositing particles. Similar results had been observed in the studies of dispersion from a source at $x_2 = 40$.

The time variation of the number of particles in the field is presented in Fig. 13a and the rates of deposition, in Fig. 13b. The average velocities of the particles hitting the wall are presented in Fig. 14. The free-fall velocity is represented by a dashed line. Due to the initial conditions V_W is zero at $t = 0$. Its magnitude decreases monotonically with time and reaches a constant value, at about $t = 100$, which is almost the same as observed in Fig. 3 for the dispersion of particles from a source at $x_2 = 40$. However, the results shown in Fig. 14 differ from those in Fig. 3 in that particles start to deposit immediately after the start of the process. This is because they are distributed uniformly at $t = 0$. Those arriving at the wall, therefore, start their free-flight to the wall at a number of locations, where the magnitudes of the turbulent velocity fluctuations can be quite different. Thus, the average values of V_W in Fig. 3 are much larger at small times. The model is seen to give smaller values of V_W than is observed in the DNS. This is reflected in the smaller rates of deposition shown in Fig. 13b. At $t = 500$ the model and the DNS give the same deposition rates. This occurs because the larger V_W obtained with the DNS is counterbalanced by a smaller concentration near the wall.

The root-mean-square of the fluid velocity fluctuations seen by the particles are presented in Fig. 15. The results from the DNS are represented by solid curves and the Eulerian values are represented by curves with dots and dashes. The turbulence, seen by the particles in the model

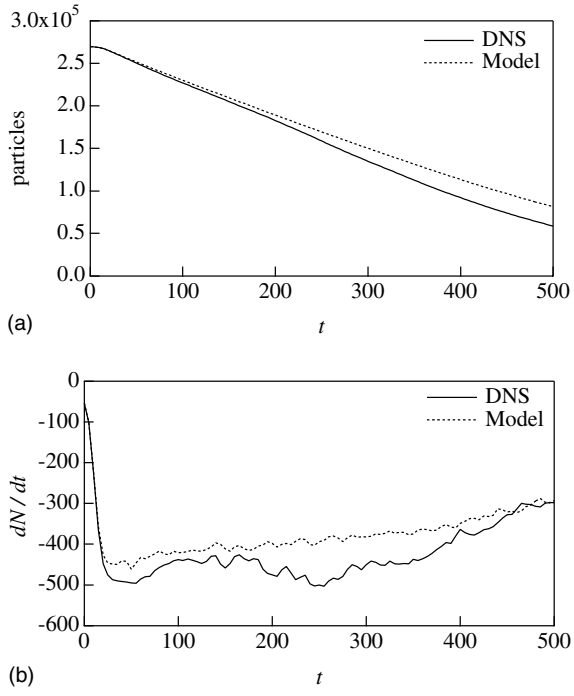

Fig. 13. (a) Particles remaining in the flow for dispersion of uniformly distributed particles. (b) Rate of deposition of particles for dispersion of uniformly distributed particles.

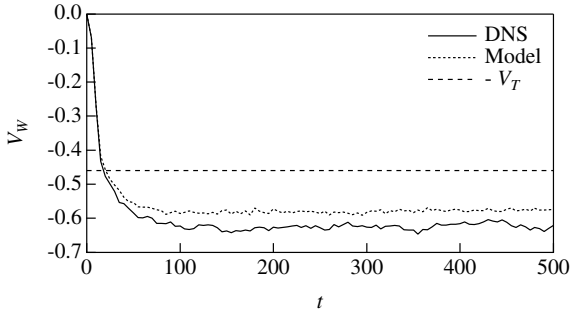

Fig. 14. Average velocity of particles depositing on the wall for dispersion of uniformly distributed particles.

calculations, is roughly the same as the Eulerian turbulence. This is not surprising since the covariance of the forcing function is selected, through Eq. (12), to provide this behavior for a Gaussian representation of $d\mu_i$. The experiments in the DNS show a difference from the Eulerian statistics, in that the particles in the model see larger fluid turbulence at $190 < x_2 < 280$ than the particles in the DNS. This is consistent with the explanation, given earlier, for the differences for concentration profiles at large x_2 shown in Fig. 12.

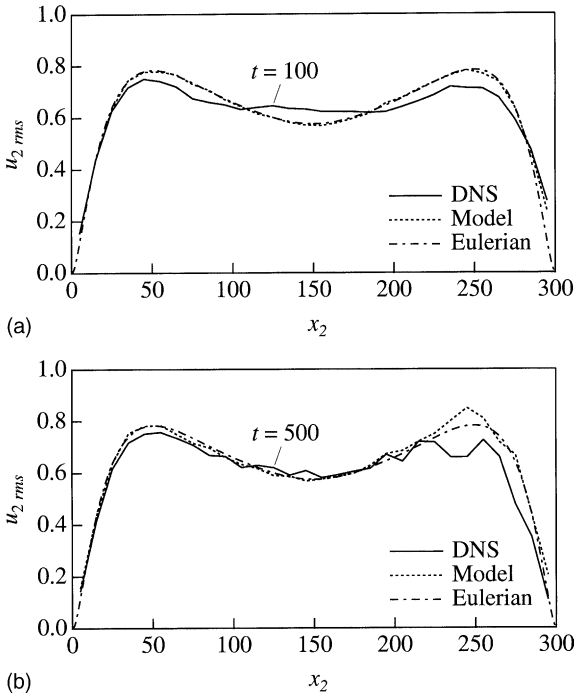

Fig. 15. Ensemble root-mean-squares of wall-normal fluid velocity fluctuations seen by solid particles conditional on the particle positions for dispersion of uniformly distributed particles.

7. Discussion and conclusions

The Langevin equation is used to describe fluid velocity fluctuations seen by the particles by making the simplifying assumptions that (1) the forcing function is Gaussian and (2) that the time scales of the fluid velocity fluctuations are same as was found by Mito and Hanratty (2002) for dispersing fluid particles. The conditions selected for the study were such that particles have a significant free-fall velocity ($V_T = 0.46$), an inertial time constant ($\beta\tau_{LF} = 1.7$) that allows the particles to have turbulence intensities which are slightly smaller than the fluid and a ratio of the stopping distance to the thickness of the viscous wall layer ($\beta^{-1} = 20$) that allows the particles to move in free-flight through a large region close to the wall. The selected value of β indicates that particles released from a rest position would reach a velocity close to free-fall at $t = 50$. Two experiments were considered: dispersion from an instantaneous point source located at $x_2 = 40$ and the settling of particles that are uniformly distributed at $t = 0$. The field is fully developed turbulent flow in a channel.

Considering the simplicity of the model and the simplicity of the assumptions used in its implementation, the agreement with experiments performed in a DNS is very good. Two differences are that the model slightly underpredicts the velocity with which the particles hit the wall and slightly overpredicts turbulent dispersion in the outer flow. The first of these leads to an underprediction of the rate of deposition for a given concentration at the wall. The second results in the

prediction of larger concentrations at larger x_2 in the experiment on the settling of a uniform distribution of particles. The reasons for these discrepancies are not understood.

The model correctly predicts that the magnitude of the deposition velocity in a turbulent field is larger than the free-fall velocity of the particles. However, Figs. 3 and 14 show that the model predicts a smaller effect of turbulence. One possible explanation is that the prediction could be improved by choosing different time scales. Calculations aimed at demonstrating this were not conclusive, mainly because the calculations were not very sensitive to changes in the time scales. Another explanation is that the assumption of a Gaussian forcing is an oversimplification. The inclusion of skewness and flatness could result in the prediction of a larger number of particles in the viscous wall layer that can move in free-flight to the wall. This was partially explored in calculations in which skewness was considered and the triple correlation in Eq. (12) was not set equal to zero. These changes did not produce an explanation of the effects that were observed.

It seems that the most likely explanation of the discrepancies is that the model is too simple to capture influences of turbulence structure. For example, the interaction between the particles and the structure could produce larger free-fall velocities in a turbulent field than would be observed in a stagnant field (Maxey, 1987; Wang and Maxey, 1993).

Acknowledgements

This work is supported by the DOE under grant DOE DEFG02-86ER13556. The calculations were done at the National Center for Supercomputing Applications located at the University of Illinois.

References

Binder, J.L., Hanratty, T.J., 1991. A diffusion model in droplet deposition in gas liquid annular flow. Int. J. Multiphase Flow 17, 1–11.

Binder, J.L., Hanratty, T.J., 1992. Use of Lagrangian statistics to describe drop deposition and distribution in horizontal gas liquid annular flows. Int. J. Multiphase Flow 18, 803–820.

Binder, J.L., Hanratty, T.J., 1993. Use of Lagrangian statistics to describe slurry transport. AIChE J. 39, 1581–1591.

Clift, R., Grace, J.R., Weber, M.E., 1978. Bubbles, Drops and Particles. Academic Press, San Diego.

Du, S., Sawford, B.L., Wilson, J.D., Wilson, D.J., 1995. Estimation of the Kolmogorov constant (C_0) for the Lagrangian structure function, using a second-order Lagrangian model of grid turbulence. Phys. Fluids 7, 3083–3090.

Durbin, P.A., 1983. Stochastic differential equations and turbulent dispersion. NASA Reference Publication 1103.

Durbin, P.A., 1984. Comment on papers by Wilson et al. (1981) and Legg and Raupach (1982). Boundary Layer Meteorol. 29, 409–411.

Friedlander, S.K., 1957. Behavior of suspended particles in a turbulent fluid. AIChE J. 3, 381–385.

Hall, C.D., 1975. The simulation of particle motion in the atmosphere by a numerical random walk model. QJR Met. Soc. 101, 235–244.

Hunt, J.C.R., Nalpanis, P., 1985. Saltating and suspended particles over flat and sloping surfaces. In: Proc. of Int. Workshop on the Physics of Blown Sand 1, 9, Memoirs, no. 8, University of Aarhus.

Iliopoulos, I., 1998. A stochastic Lagrangian model for nonhomogeneous nonGaussian fluid turbulence and its application to study particle dispersion in horizontal channel flow. Ph.D. thesis, University of Illinois, Urbana, Illinois.

Iliopoulos, I., Hanratty, T.J., 1999. Turbulent dispersion in a nonhomogeneous field. J. Fluid Mech. 392, 45–73.
Kontomaris, K., Hanratty, T.J., McLaughlin, J.B., 1992. An algorithm for tracking fluid particles in a spectral simulation of turbulent channel flow. J. Comput. Phys. 103, 231–242.
Legg, B.J., Raupach, M.R., 1982. Markov-chain simulation of particle dispersion in inhomogeneous flows: the mean drift velocity induced by a gradient in Eulerian velocity variance. Boundary Layer Meteorol. 24, 3–13.
Lillegren, L.D., 1993. The effect of a mean velocity gradient on the streamwise velocity variance of a particle suspended in a turbulent flow. Int. J. Heat Mass Transfer 19, 471–484.
Lyons, S.L., Hanratty, T.J., McLaughlin, J.B., 1991. Large scale computer simulation of fully developed turbulent channel flow with heat transfer. Int. J. Numer. Methods Fluids 13, 999–1028.
Maxey, M.R., 1987. The gravitational settling of aerosol particles in homogeneous turbulence and random flow fields. J. Fluid Mech. 174, 441–465.
McCoy, D.D., Hanratty, T.J., 1977. Rate of deposition of droplets in annular two-phase flow. Int. J. Multiphase Flow 3, 319–331.
Mito, Y., Hanratty, T.J., 2002. Use of a modified Langevin equation to describe turbulent dispersion of fluid particles in a channel flow. Flow, Turbul. Combust. 68, 1–26.
O'Brien, M.P., 1933. A review of the theory of turbulent flow and its relation to sediment transport. Trans. Am. Geophys. Union 14, 487–491.
Pan, L., Hanratty, T.J., 2002. Correlation of entrainment for annular flow in horizontal pipes. Int. J. Multiphase Flow 28, 385–408.
Perkins, R.J., 1992. The entrainment of heavy particles into a plane turbulent jet. In: Sommerfeld, M. (Ed.), Proceedings of the 6th Workshop on Two-phase Flow Predictions, Erlangen, pp. 18–33.
Pismen, L.M., Nir, A., 1978. On the motion of suspended particles in stationary turbulence. J. Fluid Mech. 84, 193–206.
Pope, S.B., 1994. Lagrangian modeling of turbulent flows. Annu. Rev. Fluid Mech. 26, 23–63.
Pozorski, J., Minier, J.P., 1998. On the Lagrangian turbulent dispersion models based on the Langevin equation. Int. J. Multiphase Flow 24, 913–945.
Reeks, M.W., 1977. On the dispersion of small particles suspended in isotropic turbulent fluid. J. Fluid Mech. 83, 529–546.
Reid, J.D., 1979. Markov chain simulations of vertical dispersion in the neutral surface layer for surface and elevated releases. Boundary Layer Meteorol. 16, 3–22.
Reynolds, A.M., 1997. On the application of Thomson's random flight model to the prediction of particle dispersion within a ventilated airspace. J. Wind Eng. Ind. Aerod. 67–68, 627–638.
Rouse, H., 1937. Modern conceptions of the mechanics of fluid turbulence. Trans. Am. Soc. Civil Engrs. 102, 463–505.
Sawford, B.L., 1991. Reynolds number effects in Lagrangian stochastic models of turbulent dispersion. Phys. Fluids A 3, 1577–1586.
Taylor, G.I., 1921. Diffusion by continuous movements. Proc. Lond. Math. Soc. 20, 196–211.
Tennekes, H., 1979. The exponential Lagrangian correlation function and turbulent diffusion in the inertial subrange. Atmos. Environ. 13, 1565–1567.
Thomson, D.J., 1984. Random walk modelling of diffusion in inhomogeneous turbulence. QJR Met. Soc. 110, 1107–1120.
Thomson, D.J., 1986. A random walk model of dispersion in turbulent flows and its application to dispersion in a valley. QJR Met. Soc. 112, 511–530.
Thomson, D.J., 1987. Criteria for the selection of stochastic models of particle trajectories in turbulent flows. J. Fluid Mech. 180, 529–556.
Ushijima, T., 1998. The motion of heavy particles in turbulent flow. Ph.D. thesis, University of Cambridge, Cambridge, England.
Ushijima, T., Perkins, R.J., 1998. Two point velocity correlation of a separating fluid element and a heavy particle. In: Proc. 3rd Int. Conf. Multiphase Flow, Lyon, France, June 8–12.
Vames, J.S., Hanratty, T.J., 1988. Turbulent dispersion of droplets for air flow in a pipe. Exp. Fluids 6, 529–546.
Wang, L.P., Maxey, M.R., 1993. Settling velocity and concentration distribution of heavy particles in homogeneous isotropic turbulence. J. Fluid Mech. 256, 27–68.